Quantum suppression of chaos in the spin-boson model

G. A. Finney* and J. Gea-Banacloche
Department of Physics, University of Arkansas, Fayetteville, Arkansas 72701
(Received 6 November 1995; revised manuscript received 8 May 1996)

We identify a transition to chaos in the semiclassical spin-boson model that occurs for relatively large boson fields, as one of two periodic orbits becomes unstable. We have studied the quantum dynamics in the vicinity of this transition, as characterized by (i) phase-space trajectories followed by quantum expectation values, (ii) spectra of such trajectories, (iii) subsystem entropies for the spin and boson systems, and (iv) growth of operator variances for the boson system. We find that the transition to chaos in the classical system has no apparent effect on any of these variables, in the spin-$\frac{1}{2}$ case. This is in disagreement with some claims made in earlier studies of this system. [S1063-651X(96)10106-9]

PACS number(s): 05.45.+b, 03.65.Sq, 42.65.Sf

I. INTRODUCTION

The spin-boson Hamiltonian

$$H=\tfrac{1}{2}\hbar\omega_0\sigma_z+\hbar\omega a^\dagger a+\hbar g\sigma_x(a+a^\dagger) \tag{1}$$

(where σ_i are Pauli spin matrices and $a^\dagger, a$ are boson creation and annihilation operators) may describe a number of physical systems, including a two-level atom coupled to a single mode of the quantized radiation field [1] or to its own center-of-mass motion in an atomic trap [2]. Taking expectation values in the Heisenberg equations and making a factorization assumption (i.e., $\langle\sigma_z a\rangle\simeq\langle\sigma_z\rangle\langle a\rangle$, etc.) yields the semiclassical equations

$$\dot{a}_1=\omega a_2, \tag{2a}$$

$$\dot{a}_2=-\omega a_1-gx, \tag{2b}$$

$$\dot{x}=-\omega_0 y, \tag{2c}$$

$$\dot{y}=\omega_0 x-4g a_1 z, \tag{2d}$$

$$\dot{z}=4g a_1 y, \tag{2e}$$

where $a_1=\langle a+a^\dagger\rangle/2$, $a_2=\langle a-a^\dagger\rangle/2i$, $x=\langle\sigma_x\rangle$, $y=\langle\sigma_y\rangle$, and $z=\langle\sigma_z\rangle$. The system (2) has long been known to exhibit chaos for certain values of the parameters [3]. A continuing question has been whether or not there is any signature of this semiclassical chaos in the solutions, especially the dynamics, of the full quantum problem (1) [4–8]. This is the subject of the present paper.

The system (1) is not of the ''standard'' form of most quantum chaos problems, which typically involve particles in externally prescribed potentials, but this very difference makes it interesting in the context of the hitherto relatively little studied ''dynamically driven'' systems, where new phenomena may arise due to, for instance, the nonunitary nature of each subsystem's evolution [9]. Moreover, the system (1) is the restriction to the $j=\frac{1}{2}$ subspace of the more general Hamiltonian

$$H=\omega_0 J_z+\hbar\omega a^\dagger a+2gJ_x(a+a^\dagger), \tag{3}$$

which describes, in general, a quantum rotor coupled to a quantum harmonic oscillator [Eq. (3) may also describe a collection of $N=2j$ two-level atoms interacting with the radiation field]. In some limits (if the reaction of the rotor on the oscillator and/or the quantum nature of the latter are negligible) this may be like a periodically driven rotor, which is an archetypal model for quantum chaos [10].

It has been shown by Graham and Höhnerbach (see [4(b)] for details) that a classical Hamiltonian for this problem may be written as

$$H_c=\omega_0 I_1+\omega I_2+4g\sqrt{I_2}\sqrt{J^2-I_1^2}\cos(\phi_1)\cos(\phi_2), \tag{4}$$

where I_i and ϕ_i are canonical action-angle variables and J^2 is a constant, corresponding to the total angular momentum [for correspondence with the quantum problem, $J^2=j(j+1)$ or, in terms of N equivalent two-level atoms, $J^2=(N/2)(N/2+1)$]. It can be verified immediately that the canonical equations of motion $\dot{\phi}_1=\partial H_c/\partial I_i$ and $\dot{I}_i=-\partial H_c/\partial\phi_i$ are identical to the equations (2) obtained from the factorization assumption in the quantum Heisenberg equations of motion, with the correspondence

$$\begin{aligned} a_1&=\sqrt{I_2}\cos\phi_2,\\ a_2&=-\sqrt{I_2}\sin\phi_2,\\ x&=\sqrt{J^2-I_1^2}\cos\phi_1,\\ y&=\sqrt{J^2-I_1^2}\sin\phi_1,\\ z&=I_1. \end{aligned} \tag{5}$$

In the classical problem (4), J is an arbitrary constant that can, in fact, be scaled away by redefining the coupling constant g and the boson field amplitude, as in $I_1'=I_1/J$, $I_2'=I_2/J$, and $g'=g\sqrt{J}$. For the quantum Hamiltonian (3),

*Present address: USAFA/DFP, U.S. Air Force Academy, Colorado Springs, CO 80840.

on the other hand, there is an infinite hierarchy of essentially different problems, in Hilbert spaces of different dimensionalities, associated with all possible values of the constant j, all of which lead to the same equivalent semiclassical equations (2) under the factorization assumption.

Given that the correspondence between the classical system (4) [or (2)] and the quantum system (3) is expected to be exact only in the double limit $j \gg 1$ and $I_2 \gg 1$, a very interesting question arises: At what point down the ladder of decreasing j do the uniquely quantum effects begin to blur the classical structure, in particular, the traces of the classical chaos? Or do any such traces persist even in the most nonclassical limit, the $j=\frac{1}{2}$ case? The following section summarizes some of the partial answers offered to these questions by previous workers on this problem.

II. BRIEF SUMMARY OF PREVIOUS RESULTS

Perhaps the most thoroughly established characteristic of quantum chaotic systems is the distribution of (nearest-neighbor) energy level differences, which is found to be Poissonian for classically integrable systems and of the Wigner form (level repulsion) for classically chaotic ones [10]. It was shown by Kuś [5] for the present system that in the $j=\frac{1}{2}$ limit the level distribution has neither of these forms, whereas Graham and Höhnerbach later [11] showed that the level distribution does approach the chaotic form with increasing j (their published results show an essentially Wigner-like distribution for $j=\frac{9}{2}$ already). This particular trace of classical chaos, therefore, does seem to vanish in the very small j limit, although we note that in a recent article Cibils, Cuche, and Müller [12] claim to have identified the ''seeds'' of quantum chaos in certain features of the spectrum of the $j=\frac{1}{2}$ system.

There are, however, other characteristics that may be exhibited sometimes by quantum systems whose classical counterparts are chaotic, such as, e.g., very fast growth of operator variances. This has in fact been observed in a hybrid quantum-semiclassical version of the present model (one with a quantized rotor and a classical field) by Fox [13]. Such a model has the factorization assumption intrinsically built in, so this result may be expected to hold in the large j limit of the fully quantized model. The question is whether this feature too disappears in the $j=\frac{1}{2}$ limit or whether it may still be identified there.

In a series of recent papers, Bonci *et al.* [8] have claimed that the latter is, in fact, the case. Specifically, they suggest, for the $j=\frac{1}{2}$ quantum system, a correlation between the semiclassical chaos, fast growth of some operator variances, and fast decay of the state purity for the spin and/or boson subsystem (or, equivalently, a fast increase in the corresponding subsystem entropy). We shall address these issues at length in what follows.

Finally, Graham and Höhnerbach too have claimed [4(b)] that ''prominent quantum effects in the dynamics [. . .] can be directly related to regular features of the classical dynamics for weak coupling and their change to chaotic behavior for stronger coupling.'' They single out certain features in the power spectrum of the boson mode, as well as the visibility (or lack thereof) of the well-known population inversion revivals. We shall present some comments about these ideas in the following section.

III. MAIN FEATURES OF OUR APPROACH

A. Meaningful comparisons: Importance of initial conditions

In order to be able to relate a particular feature of the quantum dynamics to the presence or absence of classical chaos, one should check for the presence or absence of that feature in the classically chaotic versus the classically regular regimes. Two criteria for comparisons may be used. One is to take as the reference nonchaotic system the rotating-wave approximation version of the model (1), known in quantum optics as the Jaynes-Cummings model (JCM). The other approach is to stay within the model (1) and vary parameters such as the coupling strength g to move from a classically chaotic to a classically regular regime. Both approaches have been used to some extent in the past.

In either approach, there is an important difficulty that needs to be recognized. Unlike the global properties of energy level distributions mentioned earlier, the dynamical properties such as growth of operator variances, system entropies, and revivals turn out to be quite sensitive to the initial condition chosen for, say, the spin system. This in itself is *not* a chaotic trait; it is exhibited as well by the rigorously nonchaotic JCM. We find that the criteria suggested by Graham and Höhnerbach [4(b)] generally fall into this somewhat ambiguous category: that is, it is possible to obtain very different power spectra and to suppress strongly (and modify substantially) the appearance of the population inversion revivals in the nonchaotic JCM already, simply by choosing different initial conditions for the spin system. Conversely, it is possible to choose initial conditions in the full spin-boson model (1) that lead to very similar quantum trajectories to those of the JCM or at any rate to trajectories whose differences cannot be unambiguously attributed to the classical chaos.

To be more specific, it has been shown by one of us [14] that for the JCM in the limit of large $\overline{n}$ (where $\overline{n}$ is the average occupation of the boson mode), all the main features of the quantum evolution can be understood in terms of the superposition of two special trajectories $|\Psi_+\rangle$ and $|\Psi_-\rangle$. The trajectory $|\Psi_+(t)\rangle$ [$|\Psi_-(t)\rangle$] is the total wave function for a system initially prepared in the state $|+x\rangle|\alpha\rangle$ [$|-x\rangle|\alpha\rangle$], where α is a boson field coherent state with a real amplitude α and $|\pm x\rangle$ is the corresponding eigenstate of the spin operator σ_x. As the two initial conditions $|\pm x\rangle$ form a basis of the spin space of states, it follows that the time evolution of any initial condition will be of the form

$$|\Psi(t)\rangle = \alpha|\Psi_+(t)\rangle + \beta|\Psi_-(t)\rangle, \tag{6}$$

with appropriate weights α and β. In particular, for the often chosen initial conditions where the spin starts out in an eigenstate of σ_z, the two weights are equal: $|\alpha|=|\beta|=1/\sqrt{2}$.

It turns out that the wave functions along the trajectories $|\Psi_\pm(t)\rangle$ remain approximation factorizable into a spin part and a boson part for a long time. Moreover, the evolution of most dynamical quantities (expectation values) along these trajectories is very simple. For instance, the boson field amplitude $\langle a\rangle = a_1 + ia_2$ basically oscillates as $\langle a\rangle_\pm \sim \exp(i\omega t \pm igt/2\sqrt{\overline{n}})$. Thus, for each of the two trajectories the power spectrum of a would have a single peak, at

$\omega \pm g/2\sqrt{n}$, whereas for any other initial condition leading to a superposition such as (6) one would observe two peaks, of generally unequal weights; equal weights and a symmetric power spectrum would result for the special initial conditions leading to $|\alpha|=|\beta|=1/\sqrt{2}$ (such as the eigenstates of σ_z mentioned earlier).

Similarly, the branches $|\Psi_{\pm}(t)\rangle$ by themselves display only very small population inversion oscillations and a ''revival'' that is qualitatively different [15] from the well-known revivals seen by Eberly, Narozhny, and Sánchez-Mondragón [16] for the initial condition $|+z\rangle$. The conventional revivals result, in fact, from *interference* between the two branches in Eq. (6) [14]. As such, their magnitude and appearance for different initial conditions can vary greatly as the weights $|\alpha|$ and $|\beta|$ are changed, from a maximum interference when $|\alpha|=|\beta|=1/\sqrt{2}$ to practically no revival as $|\alpha|$ or $|\beta|$ approach 1.

In a recent publication [17], we have established that, in fact, a decomposition of the same form as (6) holds for the full spin-boson system (1) (that is, in the nonintegrable, nonrotating-wave approximation case) with generally very similar properties. Specifically, we showed that (i) there are special initial states of the spin, which in [17] we called $|\psi_{\pm}(0)\rangle$, which lead to approximately factorizable wave functions for long times (a point of notation: here, as in [17], we shall use ψ for a state of the spin, and Ψ for a state of the total spin plus oscillator system); (ii) the boson field evolution along these trajectories is largely monochromatic and goes as $\langle a\rangle_{\pm}\sim\exp(i\omega t\pm i\delta\omega t)$, where $\delta\omega$ is an interaction-induced detuning, similar to the one found for the JCM; and (iii) revivals of oscillations at the Rabi frequency occur for initial conditions that result in superpositions (and hence interference) of both branches as in Eq. (6).

By choosing the right initial condition one could therefore produce a quantum trajectory in the full spin-boson system having traits very similar to those found in the JCM as regards symmetric spectra and large, visible revivals: one would only have to choose $|\alpha|=|\beta|=1/\sqrt{2}$. (See [18] for a more detailed discussion of these and other related points.)

The catch is that for the full spin-boson system, unlike for the JCM, the special initial atomic states $|\psi_{\pm}(0)\rangle$ leading to quasifactorizable evolution depend on the value of the coupling constant g. Thus, as g is changed, the same initial condition can and will result in a superposition of the two branches of the form (6) with changed weights and one will see different spectra, revivals, etc. If g is changed so that the semiclassical dynamics goes from regular to chaotic, one might then be tempted to relate the observed differences to the chaos, but this, in our opinion, would be incorrect, since in general these differences can be, for the most part, eliminated simply by changing the initial condition as g is changed in such a way as to preserve the relative weights in the expression (6).

Our approach to the study of the dynamics is then as follows: In order to minimize spurious differences between trajectories computed for different values of the coupling g, we choose our initial conditions so that we always start right on one or the other of the two branches $|\Psi_{\pm}(t)\rangle$. This makes good sense as well from the point of view of searching for the closest correspondence between the quantum and semiclassical systems, since, as was explained in [17], it is for these special initial conditions that an initially factorizable state remains approximately factorizable for the longest time, and factorization is precisely what we need in order for the semiclassical system of equations (2) to describe approximately the quantum evolution as well. We have found, moreover, that these initial conditions hold the key to some important features of the classical problem and the transition to chaos in the region of relatively large $\overline{n}$, as we discuss in the remainder of this section.

B. Classical results

For the classical system (2) we have restricted ourselves to the choices of initial conditions that make the conserved quantity $x^2+y^2+z^2=1$. Thus the point representing the state of the rotor moves on a sphere of unit radius called the Bloch sphere. This is not a real restriction since, as explained in the Introduction, the actual value of $x^2+y^2+z^2$ can be scaled away by modifying the boson field amplitude and coupling constant appropriately.

Considering then the system (2), we would expect that the quantum-classical correspondence would be more nearly accurate for large values of the boson field amplitude, a_1 or a_2. (Note that, quantum mechanically, $\overline{n}=a_1^2+a_2^2-\frac{1}{2}$, where $\overline{n}$ is the average number of oscillator quanta; for the large numbers of quanta we shall be considering here, we will neglect the $\frac{1}{2}$ term.) For sufficiently large $\overline{n}$, we expect the reaction of the rotor on the oscillator to be approximately negligible, in which case an initial condition $a_1(0)=\sqrt{\overline{n}}$, $a_2(0)=0$ would evolve approximately as $a_1=\sqrt{\overline{n}}\cos(\omega t)$, $a_2=-\sqrt{\overline{n}}\sin(\omega t)$. (We shall also take the initial phase of the oscillator to be zero throughout, again with no real loss of generality.)

If, accordingly, one sets $a_1=\sqrt{\overline{n}}\cos(\omega t)$ in the subsystem (2c)–(2e) that describes the evolution of the rotor, a periodic solution (Floquet solution of characteristic exponent zero) may be found for the three-dimensional vector $\mathbf{x}(t)$. We shall call this periodic solution $\mathbf{x}_0(t)$ here; it corresponds, in fact, to two different periodic trajectories $\pm\mathbf{x}_0(t)$, since the symmetry $\mathbf{x}\rightarrow-\mathbf{x}$ holds for the incomplete system (2c)–(2e). In [17] we called these periodic orbits the ''Autler-Townes'' (AT) trajectories (see [19]). Most importantly, we showed in [17] that if the initial condition for the quantum system is chosen to be one of the special states $|\psi_{+}(0)\rangle$ or $|\psi_{-}(0)\rangle$, discussed in Sec. III A, with the oscillator initially in a coherent state of relatively large (real) amplitude α, the expectation values for the quantum system follow closely the semiclassical AT trajectories, with only minor changes such as the interaction-induced detuning mentioned above.

As for the full classical system (2), it is clear that it will not follow the AT trajectories exactly, but our numerical studies show that for sufficiently large oscillator amplitude one can always find two periodic trajectories in the neighborhood of the AT ''branches'' $(a_1,a_2,\mathbf{x})=(\sqrt{\overline{n}}\cos(\omega t),-\sqrt{\overline{n}}\sin(\omega t),\pm\mathbf{x}_0(t))$. More specifically, for any given value of the coupling constant g and any initial condition for the oscillator of the form $a_1(0)=\sqrt{\overline{n}}$, $a_2(0)=0$, with $\overline{n}$ sufficiently large (greater than 10 or so) one can find two different initial conditions for the rotor that lead to periodic trajectories for the whole system. These initial conditions may be mapped onto the quantum system

merely by making the initial rotor state $|\psi(0)\rangle$ an eigenstate of $\mathbf{J}\cdot\mathbf{n}$ along the appropriate direction in the Bloch sphere, although it is usually sufficient to just choose the nearby AT initial condition, as described in [17], in order to achieve essentially the closest possible correspondence between the quantum and the classical evolution.

The periodic orbit followed by the classical system depends both on g and on the initial oscillator quantum number $\bar{n} \equiv a_1^2(0) + a_2^2(0)$, but we found in [17] that on resonance ($\omega = \omega_0$, the only case we shall consider here), all combinations of g and $\bar{n}$ that yield the same value for the parameter

$$\epsilon \equiv \frac{g\sqrt{\bar{n}}}{2\omega} \tag{7}$$

lead also to quite similar orbits (up to small corrections of order $1/\bar{n}$). Accordingly, and again motivated by our desire to eliminate as much as possible spurious differences between the various situations to be compared, what we have done is to change $\bar{n}$ as we changed g, so as to keep ϵ constant.

Essentially, then, our methodology is to track as closely as possible one or two periodic orbits for the classical system, through the various phase spaces that are obtained as the coupling constant g is changed. This is motivated, originally, by the fact that it is near these orbits that we find near factorization of the quantum wave function and the closest quantum-classical correspondence, but it has also an unexpected bonus: We have been able to show numerically that in this region of the phase space (which does not appear to have been investigated by earlier researchers), *chaos begins, in fact, in the neighborhood of the periodic orbits* as first one and then the other become unstable when g is increased (and $\bar{n}$ is decreased accordingly) [20].

The fact that the two branches do not become chaotic for the same values of g and $\bar{n}$, but that, rather, one of them remains stable for a wide range of parameter values after the other one has become chaotic is ultimately a consequence of the fact that the symmetry $\mathbf{x} \to -\mathbf{x}$ is broken for the full system (2) [by the term proportional to x in (2b)]. This somewhat fortuitous circumstance allows us to carry out a double comparison: We may compare the quantum evolution for an initial condition in the neighborhood of the unstable trajectory before and after the instability and we can also compare both to the quantum evolution for an initial condition in the neighborhood of the *stable* trajectory to ascertain which dynamical features, if any, can be unambiguously associated with the classical chaos. The results of these comparisons are presented in detail in the following section.

IV. QUANTUM DYNAMICS RESULTS

A. The $j = \frac{1}{2}$ case

Figures 1–3 show some typical results for the quantum system (1) with the initial conditions $|\Psi(0)\rangle = |\psi_{\pm}(0)\rangle|\alpha\rangle$, where α is a harmonic oscillator coherent state with $\alpha^2 = \bar{n}$ and we choose $\bar{n}$ and g so as to keep $\epsilon = 1$. For reference, we note that for this particular value of ϵ the AT trajectories for the semiclassical system begin at $\pm\mathbf{x}_0(0) = \pm(0.483, 0, -0.876)$ on the Bloch sphere and the corresponding initial condition for the quantum rotor is

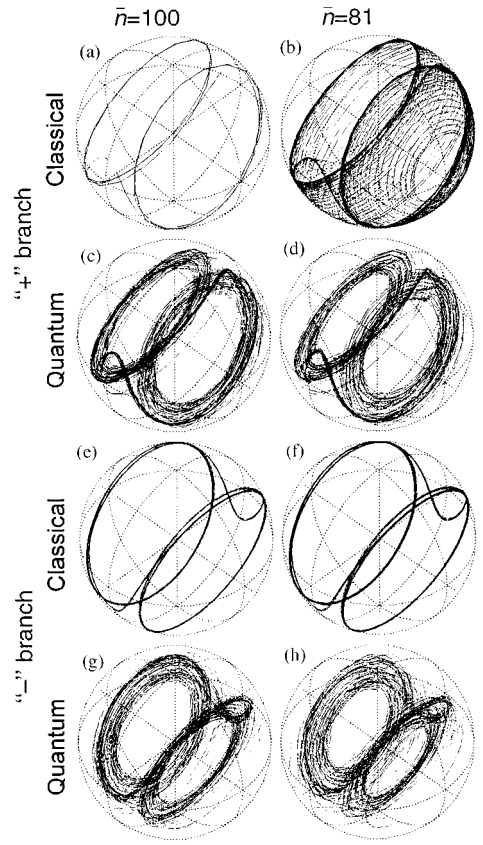

FIG. 1. Classical and quantum trajectories on the Bloch sphere (axes x, y, and z). (a)–(d) are for the chaotic (+) branch, (e)–(h) for the nonchaotic (−) branch. (a) Classical trajectory, $\bar{n} = 100$ (stable); (b) classical trajectory, $\bar{n} = 81$ (chaotic); (c) and (d) the corresponding quantum trajectories; (e) and (f) classical trajectories, − branch, $\bar{n} = 100$ and 81, respectively (both stable); (g) and (h) corresponding quantum trajectories. The total length of time shown is $\omega t = 200$.

$$|\psi_{\pm}(0)\rangle = 0.249|+z\rangle \pm 0.968|-z\rangle, \tag{8}$$

where $|\pm z\rangle$ are eigenstates of $|\sigma_z\rangle$.

Figure 1 shows a classical trajectory, in the Bloch sphere, in the neighborhood of the periodic orbit we have called the ''+'' branch, before [Fig. 1(a)] and after [Fig. 1(b)] it becomes unstable. The trajectory in Fig. 1(b) is weakly chaotic, as indicated by a calculated maximum Lyapunov exponent of $\sim 0.01 > 0$; the trajectory in Fig. 1(a) is quasiperiodic. Figures 1(c) and 1(d) are the corresponding quantum trajectories. Clearly, the quantum system is not significantly affected by the semiclassical transition to chaos; after the transition, the trajectory still remains largely in the neighborhood of the now unstable classical periodic orbit. Figures 1(e)–1(h) show for comparison the trajectories in the neighborhood of the classical orbit that does not become chaotic (− branch), both semiclassical and quantum.

The impression that the quantum system is oblivious to the classical chaos is reinforced by the spectra shown in Fig. 2 [Fourier transforms of the time series for $z(t)$]. The quantum spectra for trajectories in the neighborhood of the un-

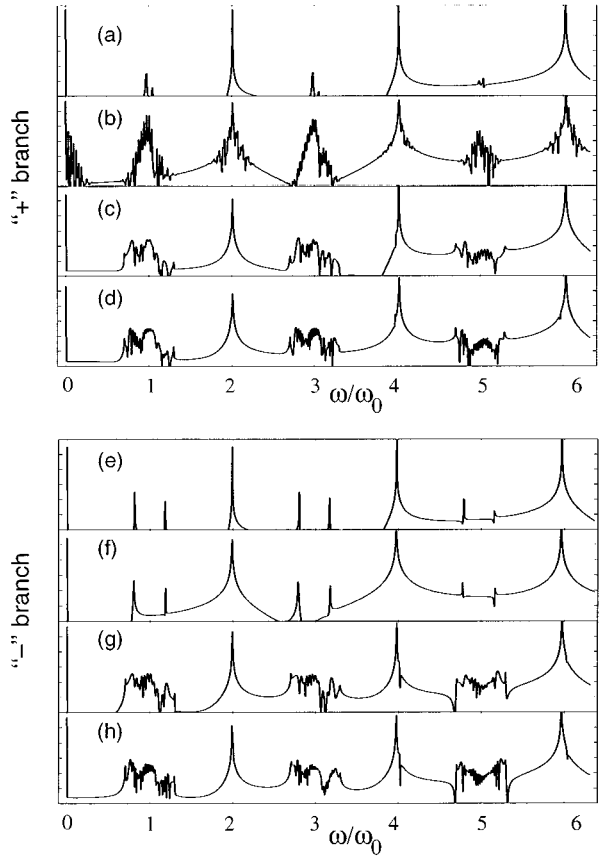

FIG. 2. Power spectra [absolute value squared of the Fourier transform of $z(t)$] for the classical and quantum trajectories, before and after the transition to chaos, both branches. Curves are labeled as in Fig. 1. The frequency resolution is $\Delta\omega = 0.008\omega_0$. The vertical scale is logarithmic, the same for all plots, and spans six decades.

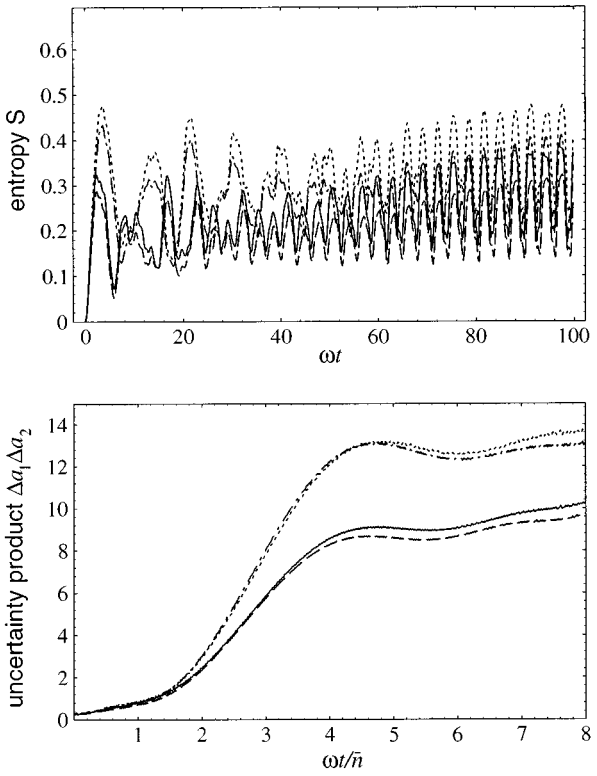

FIG. 3. (a) Entropy for the spin system and (b) uncertainty product $\Delta a_1 \Delta a_2$ for the boson field (case $j = \frac{1}{2}$). Solid line, + branch, $\overline{n} = 81$ (classically chaotic trajectory); dashed line, + branch, $\overline{n} = 100$; dotted line, − branch, $\overline{n} = 81$; dash-dotted line, − branch, $\overline{n} = 100$. The maximum possible entropy (ln2) corresponds to the upper edge of (a). The time axis in (b) has been scaled by $\overline{n}$ to account for the fact that the field uncertainty generally grows faster for smaller $\overline{n}$.

stable orbit look essentially the same as those in the neighborhood of the stable one, both before and after the classical transition to chaos.

Incidentally, Fig. 2 shows how the destabilization of the classical orbit takes place. The spectrum in Fig. 2(a) is for a quasiperiodic trajectory, since the initial condition is not exactly on the periodic orbit; it is, however, close enough that the additional frequencies seen in the spectrum can be identified with the Floquet exponents for the linearization of the system (2) around the periodic trajectory. Two of these exponents, which are imaginary and complex conjugates of each other (corresponding to real frequencies), approach zero and merge at some point between Figs. 2(a) and 2(b); these correspond to the peaks seen in Fig. 2(a) around the frequency $\omega = \omega_0$. Presumably, after merging at zero the characteristic exponents migrate along the real axis, one of them becoming real and positive and resulting in the instability observed.

Figure 2(e) shows also a double peak near $\omega = \omega_0$ for a quasiperiodic trajectory in the neighborhood of the stable periodic orbit in the − branch, but here the two peaks remain distinct as $\overline{n}$ is decreased below $\overline{n} = 90$ [Fig. 2(f)]. We have been able to establish analytically [18], using perturbation theory around the Autler-Townes orbits, that in the $\overline{n} \to \infty$, $\epsilon = \text{const}$ limit, the rate of separation of the two Floquet characteristic exponents as $\overline{n}$ is varied has opposite signs for the two branches; that is, initially, as $\overline{n}$ is decreased, the two peaks move closer along one branch but move away along the other branch. This asymmetry explains why one of the branches always becomes unstable before the other one.

As we mentioned in Sec. II, some authors have suggested that the quantum entropy of the two subsystems (spin and field) might grow faster in a semiclassically chaotic region, and similarly for the variances of some operators (notably the field uncertainty product $\Delta \equiv \Delta a_1 \Delta a_2$) [8]. Even in the nonchaotic Jaynes-Cummings model, the evolution of these quantities is very sensitive to the initial conditions chosen, with growth being generally minimized when the initial condition is the starting point for one of the $\pm \mathbf{x}_0(t)$ trajectories, as we have chosen here. With these initial conditions, Fig. 3 shows no correlation between entropy and/or uncertainty growth and chaos. Both the entropy and the uncertainty product do grow faster for the smaller values of $\overline{n}$ (which also imply larger g), but they do so for both the chaotic and the nonchaotic branch and, in any event, they do so in the nonchaotic JCM as well. [For the uncertainty product, in particular, the general arguments sketched in [14] and [21] suggest the scaling with $\overline{n}$ that we have adopted in Fig. 3(b).] If anything, Fig. 3 shows the opposite of what Bonci *et al.* [8] claimed: namely, that the entropy and uncertainty are, in

this particular example, actually *higher* for the nonchaotic branch [the dotted line, corresponding to the trajectory in Fig. 1(h)].

For the case we have chosen here, which is characterized by $\epsilon=1$, the $-$ branch remains orbitally stable as $\overline{n}$ is decreased down to $\overline{n}=32$, whereas the chaos in the neighborhood of the $+$ branch grows stronger with decreasing $\overline{n}$, as indicated by more complicated spectra and larger Lyapunov exponents. Throughout this range ($90\geqslant\overline{n}\geqslant 32$), however, the corresponding two quantum trajectories do not exhibit any significant differences that correlate with the classical chaos in any particular way. By the time $\overline{n}=32$, the factorization assumption does not hold, except for very short times, and the quantum trajectories, for both branches, only bear a passing resemblance to the classical periodic orbits.

While our results contradict the expectations of Bonci *et al.* and also, to some extent, bring into question some of the claims of Graham and Höhnerbach, they are consistent with the conclusions of other authors who, in the study of other dynamical properties (such as, e.g., Husimi functions [6]), have concluded that the quantum phase space of the $j=\frac{1}{2}$ system is considerably more robust than the classical one and that the signatures of the classical chaos are rather hard to find, if not, as we believe, entirely suppressed.

A remark may be added here regarding the size of $\overline{n}$, the number of oscillator quanta. We believe that conclusions based on the study of systems with very low values of $\overline{n}$ are suspect in general because of the lack of a good quantum-classical correspondence in that limit even in the absence of classical chaos. We have therefore tried to use values of $\overline{n}$ of large as we could and found that even for large $\overline{n}$ it is possible to find chaos in the classical system, provided that g is large enough. In this way we have identified a chaotic regime for this model that does not appear to have been studied before. We have not, however, seen any evidence that increasing $\overline{n}$ might eventually lead to quantum trajectories displaying some of the characteristics of the classical chaos [22]. Increasing $\overline{n}$ with fixed coupling g does yield better and better agreement between the classical and quantum trajectories for longer and longer times, but it also makes the chaos disappear. In a sense, the chaos takes advantage of the existence of a region of parameter space where the agreement between the quantum and the classical dynamics is still close (as Fig. 1 indicates), yet sufficiently relaxed for the classical system to become chaotic without anything noteworthy happening to the quantum system.

B. Some results for larger j

While there appears to be no identifiable limit, for the $j=\frac{1}{2}$ case, where the classical chaos might be relevant to the quantum dynamics, it has been established (see, e.g., [23]) that the factorization assumption, and hence the classical equations (2), must hold for the general system (3) for sufficiently large values of $\overline{n}$ *and* j, the total angular momentum of the rotor.

Studies on a hybrid quantum-semiclassical version of this model (quantized rotor, classical field), which has the factorization assumption built in, have indeed shown a fast growth of the variances to be correlated to chaos [13], so we may expect this to be a feature of the full quantum model (3) for values of j large enough for factorization to hold. Whether the subsystem entropy will behave similarly in this limit remains an open question. We have carried out [18] a preliminary numerical investigation of the quantum model (3) with $j=1$ and $\frac{3}{2}$ and for the latter case we have indeed found marginal evidence of an asymmetry, in the transition to chaos, between the $+$ and $-$ branches, which does point in the expected direction, i.e., to higher uncertainty and higher subsystem entropy in the chaotic region. While we do not regard our results as conclusive (since, after all, the evidence presented above for the $j=\frac{1}{2}$ model could equally well be said to point about as strongly in the opposite direction), they are suggestive and we shall briefly present some of them here.

To obtain (2) from (3) one must define $x=\langle J_x\rangle/\hbar j$, etc., $a_1=(a+a^\dagger)/\sqrt{2j}$, etc., and replace g in (2) by $g'=g\sqrt{2j}$ [where g is the actual coupling constant in the quantum Hamiltonian (3)]. This means that a classical trajectory that starts off with given values for a_1^2, a_2^2, and $\mathbf{x}$ on the Bloch sphere and a given g', actually corresponds, in the quantum model with a given value of j, to a Hamiltonian with a coupling constant $\sqrt{2j}$ times smaller and to an initial condition with $2j$ times more bosons than for the $j=\frac{1}{2}$ case.

Choosing an initial condition for the spin that corresponds to a classical periodic (Autler-Townes) trajectory is slightly nontrivial for $j\neq\frac{1}{2}$. Basically, the idea is as follows. The classical starting points for the AT trajectories on the Bloch sphere are, of course, unchanged and given by the unit vectors $\pm\mathbf{x}_0(0)$. Taking $\mathbf{x}_0(0)\equiv\mathbf{n}$ to denote a particular direction in space, we can then look at the eigenstates of $\mathbf{J}\cdot\mathbf{n}$ with eigenvalues $m=j,j-1,\ldots,-j$. For $j=\frac{1}{2}$, these eigenstates are precisely the initial states $|\psi_\pm(0)\rangle$, which we introduced earlier; for $j=\frac{3}{2}$, there are four such eigenstates, corresponding to two positive and two negative branches of quantum trajectories. We have focused on the ones with maximal angular momentum ($m=\pm\frac{3}{2}$), as they seem to follow more closely, and for a longer time, the classical trajectories. For $\epsilon=1$, this yields a starting initial condition

$$|\psi_+(0)\rangle=0.015|+\tfrac{3}{2}\rangle+0.105|+\tfrac{1}{2}\rangle+0.406|-\tfrac{1}{2}\rangle+0.908|-\tfrac{3}{2}\rangle, \tag{9a}$$

$$|\psi_-(0)\rangle=0.908|+\tfrac{3}{2}\rangle-0.406|+\tfrac{1}{2}\rangle+0.105|-\tfrac{1}{2}\rangle-0.015|-\tfrac{3}{2}\rangle, \tag{9b}$$

where the states $|m_z\rangle$ are labeled by the corresponding eigenvalues of J_z.

For the case $\epsilon=1$, a classical trajectory with $a_1^2(0)=81$, $a_2^2(0)=0$ requires $\langle a^\dagger a\rangle=243$ in the $j=\frac{3}{2}$ model and a trajectory with $a_1^2=100$ requires $\langle a^\dagger a\rangle=300$. Moreover, the rotor's space is two times larger than for the $j=\frac{1}{2}$ case. Because of this large increase in computing requirements, we have not been able to follow the quantum trajectories for times as long as those shown in Figs. 1–3. The Bloch sphere trajectories themselves do not appear substantially different from the ones shown in Fig. 1 for the $j=\frac{1}{2}$ case and so we do not reproduce them here. The evolution of the rotor's entropy, on the other hand, has the suggestive form shown in

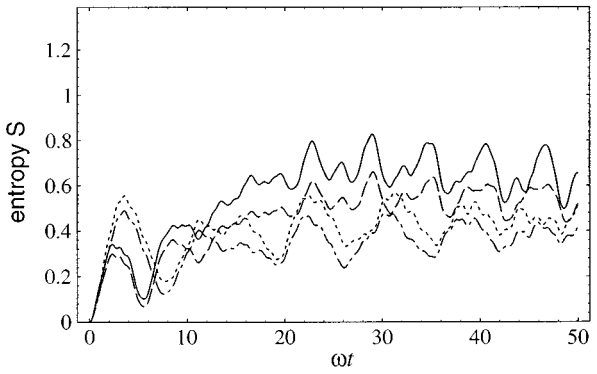

FIG. 4. Entropy for the spin system (case $j=\frac{3}{2}$). Solid line, + branch, $\langle a^\dagger a\rangle = 243$ (classically chaotic trajectory); dashed line, + branch, $\langle a^\dagger a\rangle = 300$; dotted line, − branch, $\langle a^\dagger a\rangle = 243$; dash-dotted line, − branch, $\langle a^\dagger a\rangle = 300$. The maximum possible entropy (ln4) corresponds to the upper edge of the figure.

Fig. 4. Here, contrary to what was seen in the $j=\frac{1}{2}$ case [Fig. 3(a)], the branch corresponding to the classically chaotic trajectory clearly exhibits the largest increase in entropy and this is especially true after the classical transition to chaos (solid line, + branch, $\langle a^\dagger a\rangle = 243$). This is precisely what one would expect from the arguments of Bonci *et al.* [8]. Whether it is a real effect or just a coincidence is not entirely clear to us and more work would be required to establish a positive correlation between classical chaos and growth of subsystem entropy in this model; in any event, seeing this particular effect in the $j=\frac{3}{2}$ model only makes more striking its total absence from the $j=\frac{1}{2}$ case (where the effect even appears to be reversed), which is the main point of the present paper.

We should mention also that the uncertainty product for the boson field in the $j=\frac{3}{2}$ case also displays a behavior similar to the one seen in Fig. 4 for the entropy, that is, the classically chaotic branch does grow faster, especially after the transition to chaos. However, because of the scaling with $\overline{n}$ indicated in Fig. 3(b), we have not been able to cover a very large range of times, and for those short scaled times the differences between the uncertainty products for the various branches would, in fact, be barely visible on the scale of Fig. 3(b).

V. CONCLUSION

In conclusion, we believe that in the $j=\frac{1}{2}$ subspace of the system (3) there is no correlation between any particular dynamical variable and the presence or absence of semiclassical chaos. The quantum dynamics is essentially unaffected by the classical transition to chaos, and the quantum expectation values follow the semiclassical periodic orbits more closely than the semiclassical system itself after the latter becomes chaotic, showing that these orbits remain about as stable, or as unstable, as they were before the transition, as far as the quantum system is concerned. We may therefore speak of a total quantum suppression of chaos for this system—''quantum'' because it is clearly the highly nonclassical nature of the two-level system (as compared to a classical rotor) that is responsible for this result.

ACKNOWLEDGMENT

This research has been supported by the National Science Foundation.

[1] See, e.g., C. Cohen-Tannoudji, J. Dupont-Roc, and G. Grynberg, *Atom-Photon Interactions* (Wiley, New York, 1992), and references therein (especially Complement A_{VI}).

[2] J. I. Cirac, A. S. Parkins, R. Blatt, and P. Zoller, Phys. Rev. Lett. **70**, 556 (1993); C. A. Blockley, D. F. Walls, and H. Risken, Europhys. Lett. **17**, 509 (1992).

[3] P. I. Belebrov, G. M. Zaslavskii, and G. Kh. Tartakovskii, Zh. Éksp. Teor. Fiz. **71**, 1799 (1976) [Sov. Phys. JETP **44**, 945 (1976)]. For a related system, see also P. W. Milonni, J. R. Ackerhalt, and H. W. Galbraith, Phys. Rev. Lett. **50**, 966 (1983).

[4] (a) R. Graham and M. Höhnerbach, Z. Phys. B **57**, 233 (1984); (b) in *Quantum Measurement and Chaos*, edited by E. R. Pike and S. Sarkar (Plenum, New York, 1987), p. 147.

[5] M. Kuś, Phys. Rev. Lett. **54**, 1343 (1985).

[6] L. Müller, J. Stolze, H. Leschke, and P. Nagel, Phys. Rev. A **44**, 1022 (1991).

[7] M. B. Cibils, Y. Cuche, P. Lebouef, and W. F. Wreszinski, Phys. Rev. A **46**, 4560 (1992).

[8] L. Bonci, R. Roncaglia, B. J. West, and P. Grigolini, Phys. Rev. Lett. **67**, 2593 (1991); Phys. Rev. A **45**, 8490 (1992).

[9] For a discussion of this point with a relevant example, see L. E. Ballantine, Phys. Rev. A **44**, 4126 (1991); **44**, 4133 (1991).

[10] See, e.g., F. Haake, *Quantum Signatures of Chaos* (Springer-Verlag, Berlin, 1990).

[11] R. Graham and M. Höhnerbach, Phys. Rev. Lett. **57**, 1378 (1986).

[12] M. B. Cibils, Y. Cuche, and L. Müller, Z. Phys. B **97**, 565 (1995).

[13] R. F. Fox, Phys. Rev. A **44**, 6193 (1991).

[14] J. Gea-Banacloche, Phys. Rev. A **44**, 5913 (1991); Opt. Commun. **88**, 531 (1992).

[15] Ho Trung Dung and A. S. Shumovski, Opt. Commun. **83**, 220 (1991).

[16] J. H. Eberly, N. B. Narozhny, and J. J. Sánchez-Mondragón, Phys. Rev. Lett. **44**, 1323 (1980).

[17] G. A. Finney and J. Gea-Banacloche, Phys. Rev. A **50**, 2040 (1994).

[18] G. A. Finney, Ph.D. dissertation, University of Arkansas, 1995 (unpublished).

[19] S. H. Autler and C. H. Townes, Phys. Rev. **100**, 703 (1955).

[20] We emphasize that this ''soft'' transition to chaos occurs in a regime (large $\overline{n}$, relatively small g) rather far removed from the one that has been studied quite thoroughly by R. F. Fox and J. Eidson, Phys. Rev. A **34**, 482 (1986), where the system (2) behaves like a perturbed Chirikov pendulum. With our pa-

rameters, and for the $j=\frac{1}{2}$ case, that regime would correspond to extremely small $\overline{n}$ and very large g.

[21] J. Gea-Banacloche, Phys. Rev. A **46**, 7307 (1992).

[22] This is in contrast to what has been observed for some other systems; see, e.g., X. Zheng and C. M. Savage, Phys. Rev. A **51**, 792 (1995), for a quantum-optical example.

[23] M. B. Cibils, Y. Cuche, W. F. Wreszinski, J.-P. Amiet, and H. Beck, J. Phys. A **23**, 545 (1990).